Factors Affecting Defoliation Assessment Using Airborne Multispectral Scanner Data

Donald G. Leckie
Petawawa National Forestry Institute, Chalk River, Ontario K0J 1J0, Canada

ABSTRACT: Classifications of airborne mutlispectral scanner data for forest defoliation assessment have generally met with only moderate success. Key factors affecting defoliation assessment (radiometric distortions within the imagery due to atmosphere, sun-object-viewer geometry and topography, small spectral differences between defoliation levels, spectral variability due to stand characteristics, and confusion of defoliation classes with other forest types) are examined with the aid of an example of current spruce budworm defoliation in a mixed fir and spruce forest which also contains cumulative spruce budworm defoliation. Analysis indicates that these factors can seriously affect classification of defoliation levels. For example, for certain spectral bands, radiometric distortion can be an order of magnitude larger than the difference between current spruce budworm defoliation levels, slopes of 5° to 15° can cause differences in multispectral scanner intensities equivalent to the range of intensities for areas of healthy to severe current defoliation, and 5 to 10 percent differences in the hardwood component in mixedwood stands can result in intensity differences equivalent to the differences separating defoliation levels. Confusion of current defoliation classes with mixedwood stands and stands of cumulative defoliation can be particularly severe.

INTRODUCTION

CLASSIFICATIONS of both satellite and airborne mutlispectral scanner data for accurately detecting and assessing insect and disease damage of forests have proven difficult. Damage assessments derived from Landsat Multispectral Scanner (MSS) data are often inadequate (Harris *et al.*, 1978; Madding and Hogan, 1978; Dottavio and Williams, 1983; Hall *et al.*, 1983; Nelson, 1983; Rencz and Nemeth, 1985). Insufficient spatial resolution, insufficient spectral characteristics (e.g., number of bands, nonoptimum spectral bands), and unreliability of data acquisition (due to cloud cover during optimum biowindows for the detection of damage symptoms) are often cited as the main cause of the inadequacies of Landsat MSS data.

Some improved capabilities for damage assessment may be derived from the second generation, higher resolution Earth resources satellites (Nelson *et al.*, 1984; Rencz and Nemeth, 1985; Buchheim *et al.*, 1985; Beaubien and Laframboise, 1985). The Landsat Thematic Mapper (TM) sensor has increased spatial resolution and number of spectral bands, whereas the SPOT High Resolution Visible (HRV) system has increased spatial resolution and greater reliability of acquiring cloud-free data within optimum biowindows. Airborne MSS data offer possibilities for a large number of wavebands, flexible waveband choice, flexible ground resolution, and flexibility in the timing of data acquisition. Studies investigating classification of airborne MSS data for forest damage assessment have met with variable, but generally moderate, success (Weber and Polcyn, 1972; Leckie and Gougeon, 1981; Teillet *et al.*, 1981; Koch *et al.*, 1984; Leckie and Ostaff, 1987). The main factors limiting the success of these classifications were radiometric distortions within the imagery, small spectral differences between damage types and the levels being assessed, confusion in classification with other forest types, and spectral variability of areas of similar defoliation due to differing forest stand characteristics (e.g., species, age, crown closure, and presence of other damage types).

The purpose of this study was to quantify these problems and explore solutions. Airborne MSS data of a study area exhibiting current spruce budworm (*Choristoneura fumiferana* (Clem.)) defoliation were examined in detail. The damage symptoms being classified, forest types of the study area, and airborne multispectral imagery used provide a useful data set, because the data exhibited problems common in classification of airborne MSS data for forest damage assessment.

DATA AND TEST AREA

Data Acquisition

Airborne MSS data were acquired over two test areas (Sisson Reservoir and Trousers Lake test areas) in northern New Brunswick, Canada. The data were acquired by a Daedalus model 1260 eleven channel multispectral scanner (Zwick *et al.*, 1980) mounted in a DC-3 aircraft operated by the Canada Centre for Remote Sensing. Table 1 gives the flight line and data specifications for both test areas. The wavelength bands of the scanner are given in Table 2. The field of view of the scanner was $\pm 36.9°$. Normal color aerial photographs of the test areas at 1:24,000 scale were acquired. Normal color photographs at 1:11,000 and 1:4,000 scale, color infrared photographs at 1:5,500 scale, and oblique 35-mm color photographs from 90, 180, and 490 m above ground level were obtained for selected segments of the test area. All airborne MSS data and aerial photographs were acquired 3 July 1981. A detailed sketch-map survey of defoliation in the test areas was also conducted.

Site Description

Balsam fir (*Abies balsamea* (L.) Mill.) and spruce, mainly white spruce (*Picea glauca* (Moench) Voss), were the predominant softwood species in the test area and generally occurred together in mixed stands. Eastern white cedar (*Thuja occidentalis* L.), tamarack (*Larix laricina* (Du Roi) K. Koch), and jack pine (*Pinus banksiana* Lamb.) were also present. Mixedwood and hardwood stands were common. The terrain of both test areas was flat or gently rolling, with some areas of broad hills generally less than 75 m in height.

Defoliation Conditions

Spruce budworm defoliation results in two damage symptoms: red discoloration of the foliage (current defoliation) and loss of foliage (cumulative defoliation). In the spring and early summer the budworm feeds on the buds and new shoots of balsam fir (the preferred host), white spruce, red spruce (*Picea rubens* Sarg.), and, to a lesser extent, on some other softwood species. This feeding results in red discoloration of attacked trees due to partially consumed needles adhering to a web-like structure produced by the budworm. The partially consumed needles dry out, turn a red color, and eventually fall off the tree due to wind and rain. Therefore, for a short period of time (two to three weeks) in late spring and early summer, affected trees and forest stands have a reddish hue. Successive years of current

PHOTOGRAMMETRIC ENGINEERING AND REMOTE SENSING,
Vol. 53, No. 12, December 1987, pp. 1665–1674.

0099-1112/87/5312–1665$02.25/0

TABLE 1. FLIGHT PARAMETERS

Location	Time (ADT)	Solar altitude	Solar azimuth	Flight line azimuth	Altitude AGL (m)	Ground resolution (m)
Sisson Reservoir test area (47°20'N, 67°21'W)	0935	37°	095°	220°	3650	9.1
Trousers Lake test area (47°00'N, 66°50'W)	0952	40°	099°	085°	3775	9.4

TABLE 2. AIRBORNE MULTISPECTRAL SCANNER BANDS

Band[1]	Wavelength (μm)
1	0.39 - 0.42
2	0.42 - 0.45
3	0.45 - 0.50
4	0.50 - 0.55
5	0.55 - 0.60
6	0.59 - 0.65
7	0.63 - 0.70
8	0.68 - 0.78
9	0.77 - 0.90
10	0.87 - 1.04
11	1.55 - 2.75

Note: Bands 1 and 2 were not used in this analysis due to high noise levels.

[1]Bands 1 through 10 are from Zwick *et al.* (1980); band 11 is from McColl (pers. comm.).

defoliation result in a cumulative loss of foliage and exposure of bare twigs.

All data for this study were acquired in early July during the peak period of red discoloration. Both test areas had suffered defoliation of varying intensity for numerous years. The forest condition of the Sisson test area consisted of varying degrees of current defoliation on the fir and spruce trees, with cumulative defoliation of varying degrees occurring in many stands. A single stand or tree sometimes contained both current and cumulative defoliation. Mortality also occurred. The Trousers Lake test area contained large areas of unaffected healthy forest and areas with varying amounts of cumulative defoliation. Current defoliation was minor and occurred in only small scattered areas.

PROCEDURES

Data Preprocessing

Sun-object-viewer geometry and the changing influence of atmospheric path radiance and attenuation with scan angle resulted in severe radiometric distortions along the across-track direction of the MSS imagery. The combined effects of these distortions were modeled using a least- squares fit quadratic or cubic polynomial relating mean pixel intensity values (dependent variable) of sample areas containing current and moderate cumulative defoliation (Sisson Reservoir test area) or mixed healthy fir and spruce (Trousers Lake test area) to the pixel location of the centroid of the sample areas (independent variable) (e.g., Figure 1). A separate correction curve was determined for each band of each test area and applied in an additive manner to the image of each band. The coefficient of determination of these correction curves ranged from 0.90 to 0.98 for bands of the Sisson Reservoir data and 0.75 to 0.88 for bands in the visible wavelengths of the Trousers Lake data. Coefficients of determination were lower (0.13 to 0.75) in the infrared bands of the Trousers Lake data because trends with view angle were lower and spectral variation higher. Possible biases in the Sisson Reservoir data introduced by employing stands of different defoliation conditions were minimized by using a large number of sample areas (45) which had an approximately uniform spatial distribution of the different defoliation conditions across the image. Similarly, for the Trousers Lake test area, sample areas of different spruce and fir composition were evenly distributed across the image. Due to insufficient data and the instability of the polynomial fits near the edges of the images, the shapes of the correction curves at large look angles were questionable, and data within 100 pixels (28°) of either edge of the images were not used in the analysis.

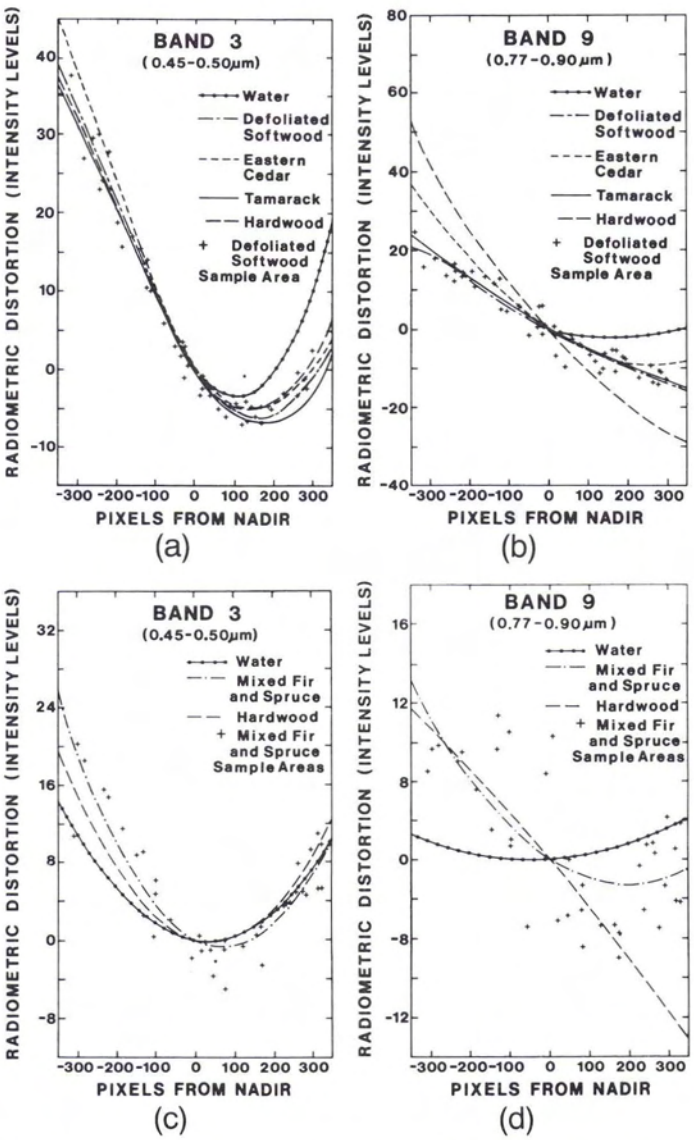

FIG. 1. Radiometric distortion across band 3 (blue) and band 9 (near-infrared) images. The lines represent the polynomial correction curves for each surface type derived from the relationship of mean pixel intensity value versus pixel location (centroid) of each sample area. The mean intensity value for sample areas of defoliated mixed fir and spruce (Sisson Reservoir data) and healthy mixed fir and spruce (Trousers Lake data) are plotted. The scanner is viewing the predominantly sunlit side of the trees for negative pixels from nadir. (a) Sisson Reservoir. (b) Sisson Reservoir. (c) Trousers Lake. (d) Trousers Lake.

Developing Ground Reference Data

Sample areas consisting of forest stands or segments of stands with similar defoliation condition were defined. These areas were of pure, generally mature, dense fir/spruce to spruce/fir composition. Their size generally ranged from 100 to 1,000 pixels. Sample areas with different stand characteristics were also selected.

Photointerpretation of the aerial and oblique photographs was used to determine the defoliation levels of sample areas. Current defoliation was assessed by the intensity of red coloration and the proportion of trees with red discoloration. Species composition of sample areas was also determined by photointerpretation supported by forest inventory map data.

The defoliation condition of sample areas was assessed according to two systems. The first system was used to quantify current or cumulative defoliation in order to analyze spectral differences due to defoliation. To facilitate analysis of spectral differences due to current defoliation, sample areas with only current defoliation were selected and their defoliation level assessed according to a rating system between 0 and 20 for healthy through to very severe current defoliation (0 to 5 representing healthy and minor defoliation, 5 to 10 light, 10 to 15 moderate, and 15 to 20 severe defoliation). Areas with cumulative defoliation were also selected and cumulative defoliation rated according to a similar system. However, due to the presence of various levels of current defoliation (severe to healthy) associated with the cumulative defoliation, stands of similar ratings may have very different defoliation conditions.

A second defoliation categorization system was developed to test the capabilities to digitally classify different defoliation levels. Defoliation classes were defined as follows:

- healthy - no visible current or cumulative defoliation and no mortality;
- light defoliation - current defoliation less than 35 percent[1]; generally having less than 10 to 15 percent[2] cumulative defoliation;
- moderate defoliation - current defoliation 35 to 70 percent; generally having less than 20 percent cumulative defoliation;
- severe defoliation - current defoliation greater than 70 percent; generally having less than 20 percent cumulative defoliation; and
- cumulative defoliation - 25 to 100 percent cumulative defoliation but generally between 25 and 60 percent; the other component of the forest may be current defoliation and/or healthy; the term moderate cumulative defoliation will be used for stands of 25 to 60 percent cumulative defoliation.

Analysis Procedures

Radiometric Distortions. The magnitude and nature of radiometric distortions across airborne MSS imagery were examined for several forest types for the two flight lines of the test data set of this study. The distortions in each spectral band were estimated from plots of the mean of sample areas of each forest type versus the position of the sample areas relative to nadir (e.g., Figure 1). The distortion for water surfaces was used to approximate path radiance and to assist in indicating the contribution of sun-object-viewer geometry to the radiometric distortion of the forested surfaces. Several empirical techniques (modeling scene statistics and ratioing of bands) were tested as simple methods for correcting radiometric distortions across the image.

An approximation of radiometric distortions due to slope and aspect for the data of this study was calculated using a Lambertian model of the forest canopy. A simple correction was applied to the data for path radiance, based on the intensity recorded over a water surface and assuming a low water reflectance.

[1] The percent current defoliation is estimated from the proportion of the visible portion of the tree crowns of the sample area with a red coloration and the intensity of that red coloration.

[2] The percent cumulative defoliation is the proportion of foliage lost from the visible portion of the tree crowns of the sample area.

Spectral Differences Among Current Defoliation Levels. The spectral differences among current defoliation levels were characterized by analyses of the means and standard deviations of homogeneous defoliated sample areas. The mean pixel intensity of sample areas (Sisson Reservoir test area) for the nine spectral bands was plotted against current defoliation rating of the sample area. Similarly, the mean intensity of various features derived from the nine spectral bands was plotted. Examples for some of the bands and features reported to be most useful for discriminating defoliation conditions (Leckie and Ostaff, 1987) are given in Figure 2.

A problem arises in using this data set for estimating a trend in recorded intensity due to different current defoliation levels. Spruce has a higher reflectance than balsam fir in all bands (see Variable Spruce and Fir Composition subsection). Becauses the healthy stands in the Sisson Reservoir test area, including those of Figure 2, are mainly spruce/fir, with some being spruce, there is a bias towards high intensities for the healthy sample areas used in this study, and differences between healthy fir/spruce and the current defoliation stands may vary from those indicated in Figure 2. The sample areas of light, moderate, and severe current defoliation and of moderate cumulative defoliation are not biased towards greater or fewer numbers of spruce/fir or fir/spruce sample areas. Thus, although variability among stands of a similar defoliation level was increased by including stands of compositions of spruce/fir through to fir/spruce, trends of intensity with defoliation level were not unduly biased. A typical range of intensities for healthy stands of varying proportions of spruce and fir was estimated in Figure 2 by using the data of Figure 3. Taking the classification training area as a typical stand of spruce/fir, the expected intensity of stands with other fir and spruce compositions was estimated by (1) determining the differences between the intensity of stands of other composition and the spruce/fir of Figure 3, and (2) adding these differences to the intensity of the classificaiton training area. This range shows the mean intensity expected as the composition of healthy stands (Figure 3) varies from pure spruce (upper end of range) through to pure balsam fir (lower end of range). When estimating trends of intensity with current defoliation level by comparison of healthy stands with sample areas with defoliation, the middle part of the range corresponding to fir/spruce - spruce/fir was used.

A maximum likelihood classification of the Sisson Reservoir test area using all spectral bands was conducted (1) to determine the levels of defoliation which can be reliably separated and (2) to characterize confusion of defoliation classes with other forest types. Representative sample areas of each of the four current defoliation classes (classification training areas) were used to generate the class statistics for the maximum likelihood classifier. Other classes (moderate cumulative defoliation, eastern cedar lowlands, tamarack, and three mixedwood) were also classified. Accuracy was assessed by comparing the classification results with a test data set of independent sample areas.

Spectral Variability Due to Stand Characteristics. The problem of spectral differences among areas of similar current defoliation level but different forest stand characteristics was quantified by examining the spectral differences among pixels containing varying quantities of other forest types (e.g., Figures 2, 3, and 4) and relating these differences to the spectral differences among defoliation classes. The cases of cumulative defoliation mixed with current defoliation, variable fir and spruce composition, and presence of a hardwood component in a defoliated stand were quantified, and spectral bands or band ratios useful in minimizing the effects of these variables were determined. As well, age and crown closure are discussed because these factors account for spectral differences among areas of similar defoliation condition.

Confusion of Current Defoliation with Other Forest Types. Confusion of current defoliation with other forest types was determined. The confusion with cumulative defoliation was estimated using

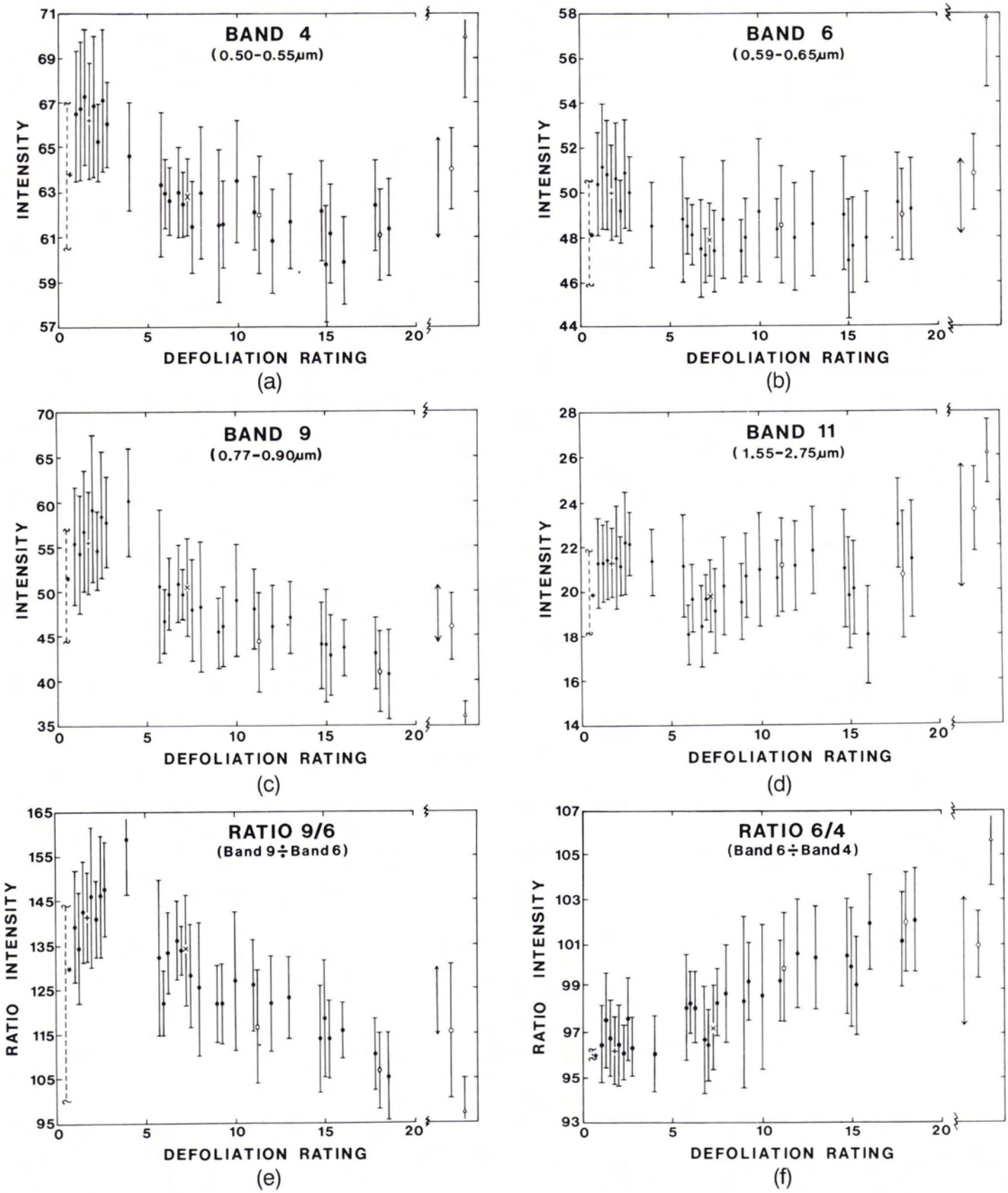

FIG. 2. Spectral signatures (band 4, 6, 9, and 11) and band ratios (9/6 and 6/4) versus current defoliation level. Mean intensity level and standard deviation for dense fir/spruce to spruce/fir sample areas. Defoliation is rated from 0 to 20 (0 to 5 = healthy and very light, 5 to 10 = light, 10 to 15 = moderate, 15 to 20 = severe). Also given is the range of mean intensity levels for 21 moderate cumulative defoliation sample areas (↕), the mean intensity level for a severe cumulative defoliation (total defoliation) sample area (Δ), and the mean intensity levels for the classification training areas (healthy +, light x, moderate □, severe ◇, moderate cumulative defoliation ○); the typical range of intensity levels resulting from a varying spruce and fir component of a healthy stand (⟊) based on the classification training area for the healthy class (+) being typical of a spruce/fir stand; and the estimated intensity for a healthy fir/spruce - spruce/fir stand (*).

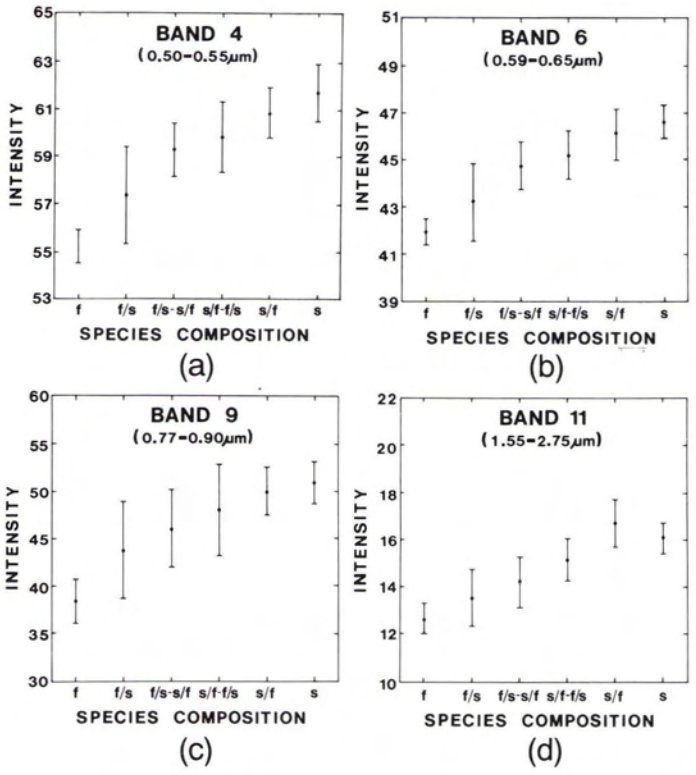

FIG. 3. Spectral signatures (bands 4, 6, 9, and 11) versus species composition [balsam fir (F) to spruce (S)] for healthy stands of the Trousers Lake test area. Absolute intensity values of these data are not comparable with those of the Sisson Reservoir test area but the irradiance increments represented by the intensity levels are approximately equivalent. Forty-six sample areas were used.

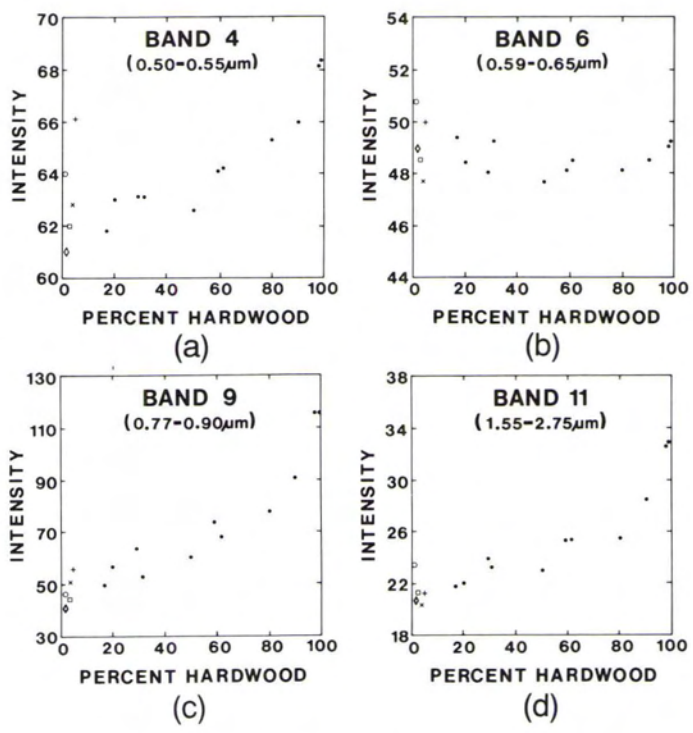

FIG. 4. Mean intensity value recorded by the airborne multispectral scanner (bands 4, 6, 9, and 11) for sample areas of different softwood/hardwood composition in the Sisson Reservoir test area. The softwoods generally had moderate current defoliation with some areas of cumulative defoliation. To minimize the effects of differing radiometric distortion correction curves for softwoods and hardwoods, sample areas were selected from a region between pixel 25 and 125, near the portion of the correction curves where the slopes are smallest and the curves of softwood and hardwoods are similar (Figure 1). Also, the mean intensity levels for the five classification training areas are indicated, using the symbols of Figure 2, in order to provide comparison (approximate due to different correction curves) with the mixedwood stands.

overlap of spectral signatures and confusion in classification results. Spectral bands useful in reducing this confusion are discussed. Confusion with other forest types was also estimated from classification results.

ANALYSIS OF FACTORS AFFECTING CLASSIFICATION OF DEFOLIATION

Radiometric Distortions

Radiometric Distortions Across the Imagery. Radiometric distortions across a forested image are influenced largely by changes in several key parameters with view angle: path radiance and atmospheric attenuation, bidirectional reflectance of the objects being viewed, and the components of the forest being viewed (e.g., more ground cover and understorey is viewed near nadir than at large view angles where the upper portions of the forest canopy often dominate the field of view of the scanner). Figure 1 gives examples of the form and magnitude of the radiometric distortions of the two data sets of this study (Table 1).

Assuming the reflectance of water to be low and diffuse for the angles of view of the scanner, most of the variation in water intensities observed across the image (Figure 1) can be attributed to path radiance. It is apparent that path radiance contributed to the increase in intensity near the edge of the images of the visible spectral bands and was the main cause of the increased intensities on the side of images acquired looking towards the sun (i.e., viewing backlit trees). There was no increase in recorded infrared intensity near the backlit edge of the image. Atmospheric attenuation and path radiance effects are small in the infrared wavebands, and distortions in the infrared bands were largely due to the effects of sun-object-viewer geometry (e.g., Figures 1b and 1d). The larger magnitude of change with view angle and greater asymmetry of the curves of Sisson Reservoir versus Trousers Lake is due to stronger sun angle effects for the Sisson Reservoir data, which had a 55° difference between sun and flight line azimuth as opposed to a 14° difference for the Trousers Lake data. The effect of sun-object-viewer geometry, therefore, can contribute greatly to radiometric distortion in both the visible and infrared parts of the spectrum. Results of reflectance modeling and field spectral measurement studies have also demonstrated the importance of sun-object-viewer geometry (e.g., Vlcek, 1974; Kalensky and Wilson, 1975; Fox, 1978; Kimes *et al.*, 1980; Kleman, 1985; Kimes *et al.*, 1986).

The magnitudes of the radiometric distortion across an image can be large. The rates of change of image intensity with scan angle in the steepest portion of the defoliated fir and spruce curves for the Sisson Reservoir data were 1.0, 0.6, and 0.4 pixel intensity values/degree of scan angle for bands 3, 9, and 11, respectively. The distortion in some bands was an order of magnitude larger than the difference in intensity between current defoliation classes.

It is clear that radiometric distortion must be accounted for prior to or during image classification. A correction of the distortion must account for the complex nature of both the atmospheric effects and sun-object-viewer geometry effects. A modeling approach to the correction can be used. Several models have been used to correct for atmospheric effects on satellite and airborne data (Turner and Spencer, 1972; Ahern *et al.*, 1977; Potter, 1977; Selby *et al.*, 1978; O'Neill *et al.*, 1978; Woodham and Lee, 1985). These require knowledge of some atmospheric paramters and/or the following features within the image: shadow areas, clear lakes, and other surfaces of assumed spectral reflectance. Modeling of radiometric distortions across the im-

agery due to sun-object-viewer geometry effects requires knowledge of the nature of the surface and the bidirectional reflectance of the surface, as well as the influence of sky radiance. Correction procedures will, therefore, be complex.

Empirical techniques are a possible simple solution to a complex problem. A common technique is to model the radiometric distortion across the image by the variation of scene statistics across the image and then to apply an additive or multiplicative correction to the imagery based on the model. These techniques, however, are not generally appropriate for examining the subtle spectral differences which are often characteristic of forest damage. Figure 1 shows that the distortions for different surface types and, indeed, different forest types can be different. A general correction will not be sufficient. For example, for most bands of the Sisson Reservoir data, applying an additive or multiplicative correction based on one or the other of defoliated softwood or hardwood, or a mixture of the two, will lead to residual distortions remaining after the correction. An empirical correction based on one forest type is often not appropriate for other forest types, and will result in difficulties in using the data to classify other forest types. For example, with a correction based on defoliated fir and spruce, it was not possible to classify a hardwood or mixedwood class.

The ratio of bands is another possible simple correction technique, although ratios account poorly for atmospheric effects, especially path radiance. In the Sisson Reservoir data, the ratio of bands in the visible part of the spectrum eliminated most of the radiometric distortion across the imagery. For example, the ratio of bands 6 and 4 (6/4), which is a good band ratio for discriminating current defoliation, resulted in distortions of less than 1.5 intensity levels across the image for defoliated softwoods and seven intensity levels for hardwoods. Ratios of infrared bands or infrared and visible bands had important distortions. The ratio of bands 9 and 6 (9/6), also a good band ratio for current defoliation assessment, had distortions of up to 45 intensity levels across the image for both hardwoods and defoliated fir and spruce. Distortions of 12 intensity levels for defoliated fir and spruce and five intensity levels for hardwood occurred for the ratio of the mid-infrared band 11 and near-infrared band 9. Kleman (1985) computed ratios of spectral reflectance values of conifer stands acquired from a helicopter and determined that the band ratio of visible bands had less radiometric distortions due to different view angles than ratios involving a near-infrared band and mid-infrared band.

Radiometric Distortions Due to Topography. The slope and aspect of the surface is a factor in the sun-object-viewer geometry which will cause radiometric distortion. The need for correction of multispectral scanner data of forested terrain for the effect of different slopes and aspects has been documented (e.g., Sadowski and Malila, 1977; Justice, 1978; Rochon *et al.*, 1979; Smith *et al.*, 1980; Williams and Ingram, 1981).

Applying a simple Lambertian model to the data of this study indicated that slopes of approximately 15° for the blue band (4) and near-infrared bands and 5° for the red band (6) would cause a difference in recorded intensity equivalent to the range of intensities for current defoliation (severe to healthy) if the aspect of the slope is directly towards the sun. Similar values for slopes with aspects at 45° to the sun azimuth are 25° for bands 4 and 9 and 7° for band 6.

Methods of correcting for the effects of sun-object-viewer geometry in cases of different slope and aspect have been developed and function with varying degrees of success (e.g., Smith *et al.*, 1980; Hugli and Frei, 1981; Kimes and Kirchner, 1981; Teillet *et al.*, 1982; Williams and Ingram, 1981; Cavayas *et al.*, 1983). These require knowledge of the slope and aspect and add further complexity to the analysis of data.

Spectral Differences Among Current Defoliation Levels

Plots of the mean intensity of sample areas versus current defoliation rating (e.g., Figure 2) showed the near-infrared bands (bands 8, 9, and 10), and to some extent band 4 (0.50 to 0.55 μm) and perhaps band 5 (0.55 to 0.60 μm), to have a consistent trend of decreasing reflectance from healthy through to severe defoliation. There was little difference in the reflectance of different defoliation levels in the blue (band 3), red (band 6 and 7), and mid-infrared (band 11). The trends of decreasing near-infrared and green band intensities with increasing current defoliation are consistent with what might be expected due to the nature of current defoliation. Teillet *et al.* (1985) give the spectral reflectance for the various components of defoliated trees (current year needles, old needles, bare twigs, and red feeding debris). Consumption of the needles on the current year shoots during budworm feeding should cause a decrease in green reflectance. New needles, which have a considerably higher green reflectance than older needles, most bare bark, or red feeding debris, are removed or partially consumed and turn a red color. A decrease in near-infrared reflectance is expected due to the loss of foliage and low near-infrared reflectance of bare twigs and feeding debris. An increase in red reflectance is expected with increasing current defoliation because both feeding debris and bare twigs have higher red reflectances than needles, and a red coloration of the trees is the main damage symptom observed by the eye from a distance. A definite increase was not observed for the red bands used (Figure 2). This may be due to the specific wavelength interval or broad nature of the wavelength bands used. An optimized wavelength band may exhibit an increase in red reflectance. A study, which compared visual interpretations of airborne MSS (Daedalus 1260) data with those of a pushbroom multispectral scanner (MEIS II), determined that the narrower red band (0.66 to 0.69μm) of the MEIS II was the main reason for a better current defoliation assessment capability of the MEIS II imagery over the Daedalus MSS imagery (Ahern *et al.*, 1986). The spectral characteristics reported by Teillet *et al.* (1985) indicate that the maximum difference between the reflectance of healthy foliage and the red feeding debris of current defoliation in the visible part of the spectrum occurs in a narrow band at approximately 0.67 μm.

A key question is whether the differences in recorded intensity of stands of different current defoliation classes are sufficiently large, compared to the natural variability of reflectances of stands of mixed fir and spruce, to be discriminated from each other. The variability within a homogeneous stand, in terms of intensity level of the 9.0-m resolution data, is indicated by the sample area standard deviations of Figure 2. The standard deviations are generally large in comparison with trends in recorded intensity with defoliation level. Leckie and Ostaff (1987) used Bhattacharyya distance as a statistical measure of the capabilities of each band for separating defoliation levels and reported that the near-infrared bands had the greatest ability to discriminate current defoliation levels; the green band (4) had the next greatest separability. The ratio features had greater separability than single bands, with band ratio 9/6 having the best separability of the ratio of bands tested. Band ratios 6/4 and 11/9 also displayed high separability.

A good measure of the ability to separate current defoliation is the classification accuracy of a maximum likelihood classification. Table 3 gives results of the classification of Sisson Reservoir data using all nine bands. The separability of classes does not appear sufficient to classify four levels of defoliation. There is considerable confusion between severe and moderate defoliation. Three levels, heavy (a combination of severe and moderate), light, and health appear appropriate, yielding an overall accuracy of approximately 71 percent.

Spectral Variability Due to Stand Characteristics

Cumulative Defoliation Mixed with Current Defoliation. The range of intensities from healthy through moderate cumulative defoliation sample areas to the severe cumulative defoliation sample area of Figure 2 indicates the range of intensities possible for cumulative defoliation. Differences in amounts of cumulative

TABLE 3. CLASSIFICATION ACCURACY (PERCENT) FOR CLASSIFICATION OF TEN CLASSES USING NINE BANDS

	MAXIMUM LIKELIHOOD CLASS					
	Cumulative	Severe	Moderate	Light	Healthy	Others/Unclassified
Cumulative	63.3	5.3	11.4	2.6	0.2	17.2
Severe	6.9	68.7	18.0	2.9	0.2	3.3
Moderate	7.2	14.7	49.8	8.9	0.6	18.8
Light	0.8	3.3	14.2	71.4	4.2	6.1
Healthy	0.3	0.2	3.9	4.4	65.4	25.8
Cedar lowland	0.4	0.0	4.0	19.0	9.4	67.2
Tamarack	0.0	0.0	0.0	0.0	5.7	94.3
Softwood/hardwood	11.4	3.2	8.0	1.6	0.4	75.4
Mixedwood	0.6	0.1	4.1	3.8	0.3	91.1
Hardwood/softwood	0.1	0.0	1.3	0.6	0.1	97.9

defoliation mixed with current defoliation will cause difficulties in estimating the proper current defoliation level. Some bands will be more sensitive to presence of cumulative defoliation than other bands. There are considerable changes in recorded intensity for the near-infrared bands and blue band with cumulative defoliation (Leckie and Gougeon, 1981). Band 11 appears to have the largest difference in intensity between moderate cumulative and current defoliation (Figure 2). Therefore, the presence of cumulative defoliation will, in particular, alter spectral characteristics in these bands and reduce their effectiveness for discriminating current defoliation levels in cases where there is mixed current and cumulative defoliation.

Variable Spruce and Fir Composition. Figure 3 shows increases in recorded intensity with increasing spruce proportions in stands of spruce and balsam fir. White spruce generally appears brighter than balsam fir on aerial photographs (Sayn-Wittgensten, 1978). Yost and Wenderoth (1971) showed that the visible and near-infrared spectral reflectance of red spruce is greater than that of balsam fir. The magnitude of the potential variability among stands resulting from different spruce and balsam fir components is demonstrated in Figure 3. The importance of this variability relative to changes in recorded intensity resulting from different defoliation levels is estimated in Table 4. It is illustrated by the estimated range of intensities resulting from spruce and fir proportions varying from pure balsam fir to pure spruce (Figure 2). Variability in spruce and balsam fir species composition can, therefore, result in confusion. The confusion can be reduced by use of the band ratio features such as 6/4, 11/9, and 9/6 (Table 4) which are also useful features for discriminating defoliation condition (Leckie and Ostaff, 1987). For example, for band ratio 6/4, the range of intensity caused by differences in fir-spruce composition from pure balsam fir to pure spruce was only 0.07 times the difference in intensity between severe and healthy current defoliation. The corresponding ratio for composition changes from fir/spruce to spruce/fir was 0.05.

Variable Hardwood Composition. The influence of a hardwood component on the reflectance of defoliated stands can be estimated from Figure 4. Differences in recorded intensity for different hardwood percentages are very large in the near-infrared. Differences in intensity are not as large for band 11 but, in relation to the differences in intensity due to defoliation, differences due to changes in the hardwood component are important (Table 4 and Figure 2). For example, the differences in recorded intensity of bands 7 through 11 caused by 5 to 10 percent differences in hardwood component of a softwood or softwood-hardwood pixel will be similar to the difference separating one defoliation class from another (four classes). The green spectral bands (4 and 5) are less influenced by the hardwood component. A 25 to 35 percent difference in hardwood component of a softwood or softwood-hardwood pixel results in intensity differences similar to those among defoliation classes. Changes in intensity with varying hardwood component for bands 3 and 6 are small; the differences in intensity between the defoliation classes are, however, also minor (Table 4 and Figure 2).

Small proportions of hardwoods within stands of spruce and fir can, therefore, cause confusion of defoliation level, as well as make defoliation assessment in mixedwoods difficult. Use of

TABLE 4. SENSITIVITY OF BANDS AND SELECTED FEATURES TO CHANGES IN BALSAM FIR-SPRUCE COMPOSITION AND HARDWOOD-SOFTWOOD COMPOSITION RELATIVE TO THEIR SENSITIVITY TO CURRENT DEFOLIATION LEVELS

Feature	Approximate range for current defoliation[1]	Range relative to range for current defoliation[2]			
		fir versus spruce		softwood versus hardwood	
		F to S	F/S to S/F	0 to 100% H	0 to 50% H
3	0	~	~	~	~
4	−2.8	2.3	0.8	2.1	0.6
5	−2.6	2.2	0.8	1.8	0.5
6	0.9	5.1	3.2	0	0
7	−2.2	2.2	2.1	9.6	2.8
8	−11.0	1.1	0.6	6.4	2.0
9	−9.5	1.4	0.7	7.4	2.2
10	−10.5	1.3	0.8	5.9	1.9
11	1.1	3.5	2.0	10.9	2.9
4/3	4.5	0.6	0.4	1.7	0.6
6/4	6.0	0.07	0.05	1.4	0.6
9/6	−28.	1.4	0.4	6.4	2.1
11/4	−3.6	1.1	0.6	5.6	1.7
11/9	15.	0.05	0.04	1.6	0.9

[1]The range for current defoliation from severe to healthy (corrected for fir versus spruce composition) is determined from plots of mean intensity level of sample areas versus defoliation rating (e.g., Figure 2).

[2]Range divided by range for current defoliation. Range for fir versus spruce and hardwood versus softwood is determined from plots of mean intensity of sample areas versus fir-spruce and hardwood-softwood composition (e.g., Figures 3 and 4).

band 4 or band ratios 6/4 and 11/9 would aid in minimizing confusion (Table 4).

Variable Age and Crown Closures. Age is another factor which causes spectral differences among areas of similar defoliation condition. Spectral reflectances are generally higher for young trees than for mature trees (e.g., Koch *et al.*, 1984; Kleman, 1985). Leckie and Gougeon (1981) give an example of how this can result in difficulties in classifying cumulative spruce budworm defoliation.

The effects of varying crown closure are similar in nature to those of varying hardwood component. The magnitude and characteristics of these effects will vary greatly depending on type of ground cover, amount of understorey, and solar altitude. Data of Mead *et al.* (1979), Leckie and Gougeon (1981), Koch *et al.* (1984), and Kleman (1985) indicate that the effect is variable but can be large.

Confusion of Current Defoliation with Other Forest Types

Cumulative Defoliation. There can be considerable overlap of the reflectances of cumulative defoliation and current defoliation (Figure 2), which will cause confusion between the two. It may be possible to reduce this problem by incorporating cumulative defoliation classes into the classification. In this classification it is important to use spectral bands that can assist in the determination of levels of both cumulative and current defoliation, as well as in differentiating between cumulative and current defoliation. There is a large variability in reflectance of the moderate cumulative defoliation stands of the test area and those represented in Figure 2. This variability is due, in part, to differences in the amounts of current defoliation associated with cumulative defoliation, and varying composition of spruce and fir. It was difficult to establish the occurrence of trends in recorded intensity with severity of cumulative defoliation. However, a trend of increasing recorded intensity with increasing cumulative defoliation level was observed in the mid-infrared band (band 11). Leckie and Gougeon (1981) reported that, for the case of cumulative defoliation associated with healthy foliage in dense fir/spruce stands, there was also an increase in recorded intensity for the mid-infrared bands, as well as increases in the visible bands, and decreases in the near-infrared band as cumulative defoliation increased. There is little difference in recorded intensity of band 11 with changes in current defoliation, and the overlap of cumulative defoliation with current defoliation is not large. The mid-infrared band should, therefore, be helpful in differentiating cumulative defoliation from healthy stands or current defoliation. Leckie and Ostaff (1987) determined through feature selection procedures that the mid-infrared band (11) was best for discriminating cumulative from current defoliation. The best ratio of bands was that of bands 11 and 9 (11/9). Leckie and Gougeon (1981) determined that the blue band (3) and a near-infrared band (9) were good for separating classes of cumulative defoliation (associated with healthy foliage) from each other and from healthy stands. Nelson *et al.* (1984) indicated that a blue band and a mid-infrared band (2.06 to 2.33 μm) were best for discriminating cumulative defoliation levels. A 1.53 to 1.73-μm mid-infrared band was also important.

Considering both the analysis of spectral differences and feature selection, it appears that the most useful bands for discriminating cumulative defoliation (light, moderate, and severe) from both current defoliation and the healthy class are

- mid-infrared (band 11): good for separating cumulative from current defoliation (Figure 2) and the best band for determining moderate cumulative versus current defoliation and a healthy class (Leckie and Ostaff, 1987);
- blue band (3): good for differentiating cumulative defoliation levels (Leckie and Gougeon, 1981; Nelson *et al.*, 1984) and for separating severe cumulative defoliation from current defoliation (Leckie and Ostaff, 1987; Figure 2, this paper); and
- near-infrared (any of the three near-infrared bands, 8, 9, or 10): good for differentiating cumulative defoliation levels (Leckie and Gougeon, 1981); however, there is overlap in the reflectance of moderate cumulative and current defoliation (Figure 2).

Therefore, when cumulative defoliation is present, each of a blue, mid-infrared, and near-infrared band should be used in a classification of current defoliation to minimize errors resulting from the presence of cumulative defoliation.

Indeed, analysis of the classification results indicates considerable confusion between current defoliation and cumulative defoliation (Table 3). This confusion was largely with moderate and severe current defoliation. Approximately 17 percent of the moderate cumulative defoliation test areas were classified either as moderate or severe current defoliation. It was necessary to include a cumulative defoliation class in the classification to prevent large areas of cumulative defoliation from being incorrectly classified as current defoliation.

Other Forest Types. Another key factor influencing the classification capabilities of airborne MSS data for damage assessment is commission errors resulting from other forest types being classified as forest damage. Although it is not possible to test confusion of all possible forest types with damage, this study tests the commission errors between current defoliation and other forest types within the test area [i.e., eastern cedar lowlands, tamarack, softwood-hardwood stands (predominantly softwood), mixedwood stands (approximately equal proportions of softwood and hardwood), and hardwood-softwood stands (predominantly hardwood)]. The general problem of confusion between defoliation and other forest types is demonstrated in Table 3.

The main source of confusion between defoliation and other forest types was not areas of defoliation being classified as other forest types (only 1 to 11 percent of the current or cumulative defoliation test areas were classified as one of the other forest types), but the classification of test areas of the other forest types as one of the defoliation classes (Table 3). The estimates of confusion in Table 3 are likely overestimates because, in some cases, the pixels classified as defoliation are associated with small zones of defoliated fir and spruce, especially for the softwood-hardwood and eastern cedar lowlands test areas. In the case of pixels with mixed softwood and hardwood composition, the level or type of defoliation is unlikely to be reliably classified.

It was useful to include mixedwood classes in the classification to reduce the number of pixels of mixed softwood and hardwood composition that are classified as one of the defoliation classes[3]. However, in cases when atmospheric and sun-object-viewer geometry distortions are severe, classification accuracy of the mixedwood classes may be poor and inconsistent. For example, for classifications with classes of mixed hardwood and softwood versus classifications without these classes, the proportion of test areas classified as one of the defoliation classes decreased from 31 to 25 percent, 20 to 9 percent, and 5 to 2 percent for test areas of softwood-hardwood, mixedwood, and hardwood-softwood, respectively. It was also appropriate to include the eastern white cedar lowlands class because a large portion (37 percent) of these areas would be classified as light current defoliation if there were not a separate class for eastern cedar lowlands. Tamarack areas were partially classified as the healthy class (22 percent) if the tamarack class was not included.

SUMMARY AND CONCLUSIONS

Radiometric distortions across airborne MSS data due to atmospheric effects and sun-object-viewer geometry will cause difficulties in determining damage conditions in many operational surveys. A correction accounting for both components of the distortion will have to be applied. Furthermore, corrections

[3] Classification accuracies of the defoliation classes, as measured by the defoliation class test sample areas, are very similar whether or not the mixedwood classes and eastern cedar lowland and tamarack classes were included in the classification.

for hardwoods and softwoods often differ, so it is not generally possible to classify defoliation level in mixedwoods or to classify different forest types on imagery corrected for the radiometric distortion of softwoods or damaged softwoods. Topography can also cause radiometric distortions affecting classifications of defoliation levels.

The lack of spectral differences between the desired damage levels is a major difficulty in damage assessment. This difficulty can be partially overcome by use of optimized spectral bands. For the case of current spruce budworm defoliation, it has been determined that a near-infrared band and a green band are most useful, with a good combination of spectral bands of the Daedalus 1260 multispectral scanner being bands 9, 6, 4, and 3. The ratios of the infrared and red bands (9/6) and red and green bands (6/4) are particularly appropriate band ratio features for discriminating current defoliation (Leckie and Ostaff, 1987).

The problem of small spectral differences between damage classes is accentuated due to variability in the reflectance within and between stands of similar damage condition. Different species composition is an important source of this variability. Small differences in the amounts of hardwood within pixels can cause large differences in reflectance among pixels. Considerable variability in the intensities recorded by an airborne scanner can, therefore, occur from similar forest types exhibiting the same defoliation condition. It can be beneficial to use wavelength bands or features derived from bands which have low sensitivity to changes in hardwood component but are also sensitive to damage. For the case of current defoliation use of a green band (4), the ratio of red and green bands (6/4), or the ratio of mid-infrared and near-infrared bands (11/9) reduces the effect of varying hardwood component. This problem also makes it difficult to produce good classifications of defoliation classes in mixedwood stands. A more subtle but still important species effect, for the case of current spruce budworm defoliation, is the varying proportions of fir and spruce in mixed stands of fir and spruce. Band ratios 11/9 and 6/4 were effective in minimizing this effect. Differences in stand density and age can cause considerable spectral variability. The presence of damage other than that being surveyed can also cause variability in the recorded intensities of, for example, cumulative defoliation associated with current defoliation.

Confusion of classifications of damage level with other forest types is another major source of difficulty. For the case of current spruce budworm defoliation, confusion of current defoliation with cumulative defoliation is a serious problem. It will generally be necessary to include one or more classes of cumulative defoliation, as well as the current defoliation classes, to reduce confusion of cumulative defoliation with current defoliation. In cases where significant cumulative defoliation is present, mid-infrared (11), blue (3), and near-infrared (9) bands should be used in order to classify cumulative defoliation and discriminate it from current defoliation. A mid-infrared band (11) is particularly helpful for discriminating current and cumulative defoliation.

It will also often be necessary to include classes of other forest types to prevent areas of these forest types from being classified as damage classes. Accuracy of the classification of current defoliation in this study was improved by including an eastern cedar lowland class and several mixedwood classes.

Classification of forest damage is complicated. Difficulties arise from many factors. Procedures are available and must be used to reduce the difficulties. However, continued research is needed to further define, develop, and test these and new procedures and to determine if classification techniques are practical on a widespread operational basis.

REFERENCES

Ahern, F. J., D. G. Goodenough, S. C. Jain, V. R. Rao, and G. Rochon, 1977. Use of clear lakes as standard reflectors for atmospheric measurements. *Proc. 11th Int'l Symp. on Remote Sensing of Environment*. Ann Arbor, Michigan, pp. 731–755.

Ahern, F. J., W. J. Bennett, and E. G. Kettela, 1986. An initial evaluation of two airborne imagers for surveying spruce budworm defoliation. *Photogrammetric Engineering and Remote Sensing* 52(10):1647– 1654.

Beaubien, J., and P. Laframbroise, 1985. Digital airborne and satellite data for evaluating spruce budworm damage in Quebec. *Proc. Pecora 10*. Ft. Collins, Colorado, pp. 235–240.

Buchheim, M. P., A. L. Maclean, and T. M. Lillesand, 1985. Forest cover type mapping and spruce budworm defoliation detection using simulated SPOT imagery. *Photogrammetric Engineering and Remote Sensing* 51(8):1115– 1122.

Cavayas, F., G. Rochon, and P. Teillet, 1983. Estimation des réflectances bidirectionnelles par analyse des images Landsat: problèmes et possibilities de solutions. *Proc. 8th Canadian Symp. on Remote Sensing*. Montreal, Quebec. pp. 645–664.

Dottavio, C. L., and D. L. Williams, 1983. Satellite technology: An improved means for monitoring forest insect defoliation. *J. For.* 81(1):30–34.

Fox, L., 1978. The effect of canopy composition on the measured and calculated reflectance of conifer forests in Michigan. *Proc. Remote Sensing for Vegetation Damage Assessment*. Seattle, Washington, pp. 89–114.

Hall, R. J., G. N. Still, and P. H. Crown, 1983. Mapping the distribution of aspen defoliation using Landsat color composites. *Canadian J. Remote Sensing* 9(2):86– 91.

Harris, J.W.E., A.F. Dawson, and D. Goodenough, 1978. *Evaluation of Landsat Data for Forest Pest Detection and Damage Appraisal Surveys in British Columbia*. Inf. Rep. BC-X-182. Pacific Forestry Centre, Canadian Forestry Service. Victoria, B.C. 12p.

Hugli, H., and W. Frei, 1981. Corrections for anisotropic reflectances in remotely sensed images from mountainous terrain. *Proc. Machine Processing of Remotely Sensed Data*. West Lafayette, Indiana, pp. 363–374.

Justice, C.O., 1978. An examination of the relationships between selected group properties and Landsat MSS data in an area of complex terrain in southern Italy. *Proc. Fall Technical Meeting*, American Society of Photogrammetry. Alburquerque, New Mexico, pp. 303–328.

Kalensky, Z., and D.A. Wilson, 1975. Spectral signatures of forest trees. *Proc. 3rd Canadian Symp. on Remote Sensing*. Edmonton, Alberta, pp. 155–171.

Kimes, D.S., J.A. Smith, and K.J. Ranson, 1980. Vegetation reflectance measurements as a function of solar zenith angle. *Photogrammetric Engineering and Remote Sensing* 46(12):1563–1573.

Kimes, D.S., and J.A. Kirchner, 1981. Modelling the effects of various radiant transfers in mountainous terrain on sensor response. *IEEE Trans. on Geoscience and Remote Sensing*. 2:100–108.

Kimes, D.S., W.W. Newcomb, R.F. Nelson, and J.B. Schutt, 1986. Directional reflectance distributions of a hardwood and pine forest canopy. *IEEE Trans. on Geoscience and Remote Sensing*. 24:281–293.

Kleman, J., 1985. *The Spectral Reflectance of Coniferous Tree Stands and of Barley Influenced by Stress*. Ph.D. Dissertation, Dept. of Physical Geography, University of Stockholm.

Koch, B., U. Ammer, G. Kritikos, and D. Kubler, 1984. Untersuchungen zur beurteilung der vitalitat von fichten anhand multispektraler scannerdaten. *Fortstwissenschafteliches Centralblatt*. 103:214–231.

Leckie, D. G., and F. A. Gougeon, 1981. Assessment of spruce budworm defoliation using digital airborne MSS data. *Proc. 7th Canadian Symp. on Remote Sensing*. Winnipeg, Manitoba, pp. 190–196.

Leckie, D. G., and D. P. Ostaff, 1987. Classification of airborne multispectral scanner data for mapping current defoliation caused by the spruce budworm. *Forest Science* (in press).

Madding, R. P., and H. E. Hogan, 1978. Detection and mapping of spruce budworm defoliation in northern Wisconsin using digital analysis of Landsat data. Proc. 44th Annual Meeting of American Society of Photogrammetry. Washington, D.C. pp. 285–300.

Mead, R. A., R. S. Driscoll, and J. A. Smith, 1979. *Effect of Tree Distribution and Canopy Cover on Classification of Ponderosa Pine Forest from Landsat-1 Data*. Research Note RM-35. Rocky Mountain Forest and Range Experimental Station, USDA Forest Service.

Nelson, R. F., 1983. Detecting forest canopy change due to insect activity using Landsat MSS. *Photogrammetric Engineering and Remote Sensing* 49(9):1303–1314.

Nelson, R. F., R. S. Latty, and G. Mott, 1984. Classifying northern

forests using Thematic Mapping Simulator data. *Photogrammetric Engineering and Remote Sensing* 50(5):607– 617.

O'Neill, N. T., J. R. Miller, and F. J. Ahern, 1978. Radiative transfer calculations for remote sensing applications. *Proc. 5th Canadian Symp. on Remote Sensing*. Victoria, B.C., pp. 572–578.

Potter, J. F., 1977. The correction of Landsat data for the effects of haze, sun angle, and background reflectance. *Proc. Symp. Machine Processing of Remotely Sensed Data*. West Lafayette, Indiana, pp. 24–32.

Rencz, A. N., and J. Nemeth, 1985. Detection of mountain pine beetle infestation using Landsat and simulated Thematic Mapper data. *Canadian J. Remote Sensing* 11(1):50– 58.

Rochon, G., H. Audirac, A. Larrivée, J. Beaubien, and P. Gignac, 1979. Correction radiometrique des effets topographiques sur des images LANDSAT de territoires forestiers. *Télédétection et Gestion des Ressources* (F. Bonn, ed.). Assoc. Québécoise de Télédétection. pp. 151–163.

Sadowski, F. G., and W. A. Malila, 1977. *Investigation of Techniques for Inventorying Forested Regions. Vol. 1: Reflectance Modelling and Empirical Multispectral Analyses of Forest Canopy Components*. NASA CR-ERIM 122700-35-F1. 146 p.

Sayn-Wittgenstein, L., 1978. *Recognition of Tree Species on Aerial Photography*. Inf. Rep. FMR-X-118. Forest Management Institute, Canadian Forestry Service. Ottawa, Ontario, 97 p.

Selby, J. E. A., F. X. Kneizys, J. H. Chetwynd, and R. A. McClatchey, 1978. *Atmospheric Transmittance/Radiance: Computer Code LOWTRAN 4*, Report AFGL-TR-78-0953. Hanscom Air Force Base, Massachusetts, 100 p.

Smith, J. A., L. L. Tzeu, and K. J. Ranson, 1980. The Lambertian assumption and Landsat data. *Photogrammetric Engineering and Remote Sensing* 46(9):1183–1189.

Teillet, P. M., D. G. Goodenough, B. Guindon, J. F. Meunier, and K. Dickinson, 1981. Digital analysis of spatial and spectral features from airborne MSS of a forested region. *Proc. 15th Int'l Symp. on Remote Sensing of Env.* Ann Arbor, Michigan, pp. 883– 903.

Teillet, P. M., B. Guindon, and D. G. Goodenough, 1982. On the slope-aspect correction of multispectral scanner data. *Canadian J. Remote Sensing* 8(2):84–106.

Teillet, P. M., D. G. Leckie, D. Ostaff, G. Fedosejevs, and F. J. Ahern, 1985. Spectral measurements of tree defoliation. *Third Colloquium: Spectral Signatures of Objects in Remote Sensing*. Les Arcs, France, pp. 511–516.

Turner, R. E., and M. M. Spencer, 1972. Atmospheric model for correction of spacecraft data. *Proc. 8th Int'l Symp. on Remote Sensing of Environment*. Ann Arbor, Michigan, pp. 895– 934.

Vlcek, J., 1974. Difficulties in determining meaningful spectral signatures of forest tree canopies. *Proc. Symp. on Remote Sensing and Photo-Interpretation*. Banff, Alberta, pp. 805–810.

Weber, F. P., and F. C. Polcyn, 1972. Remote sensing to detect stress in forests. *Photogrammetric Engineering* 38(2):163–175.

Williams, D. L., and K. J. Ingram, 1981. Integration of digital elevation model data and Landsat MSS data to quantify the effects of slope orientation on the classification of forest canopy condition. *Proc. Machine Processing of Remotely Sensed Data*. West Lafayette, Indiana, pp. 352–362.

Woodham, R. J., and T. K. Lee, 1985. Photometric method for radiometric correction of multispectral scanner data. *Canadian J. Remote Sensing* 11(2):132–161.

Yost, E., and S. Wenderoth, 1971. The reflectance spectra of mineralized trees. *Proc. 7th Int'l Symp. on Remote Sensing of Environment*, Ann Arbor, Michigan, pp. 269–284.

Zwick, H. H., W. D. McColl, and H. R. Edel, 1980. The CCRS DS1260 Airborne Multispectral Scanner (MSS). *Proc. 6th Canadian Symp. on Remote Sensing*, Halifax, N.S., pp. 643–648.

(Received 18 December 1986; revised and accepted 30 July 1987)
